Spatial and temporal variability of rainfall towards watershed water resources management

Letícia Guarnier[1] and Gilberto Fonseca Barroso[2]

[1]Graduate Program of Environmental Oceanography, Federal University of Espírito Santo, Vitória, Espírito Santo, Brazil

[2]Department of Oceanography and Ecology, Federal University of Espírito Santo, Vitória, Espírito Santo, Brazil

Key points

- Rainfall spatial and temporal patterns in a coastal river basin were assessed with a geostatistical approach and climate indices.
- Extreme climate indices indicate that drought events in the upper basin threaten water security for agriculture and water supply.
- Because of extreme rainfall events with short-term duration, the lower basin becomes more prone to flooding.

Abstract

Analysis of multi-temporal and spatial trends of rainfall in a river basin is a useful tool for water resources management based on delimited hotspots of water scarcity and flooding risks. The present study aims to characterize rainfall distribution in a coastal watershed, Santa Maria da Vitória River Basin–SMVRB (Southeastern, Brazil). Data from 42 meteorological stations, from 2004 to 2017, were analyzed using kriging as a geostatistic tool. Anisotropy effects on rainfall were observed throughout the year and were related to regional/continental climate processes. From 1970 to 2017, trends in rainfall were computed using the RClimDex package with eleven extreme climate indices. The results have shown spatial and temporal rainfall variability, with drought events becoming more persistent in recent years. Water shortage causes water scarcity to sustain crops and threatening water supply. In the lower river basin, where part of the Great Vitória metropolitan area is located, flooding risks increase in the response of intensive short-term rainfall events. Knowledge of rainfall variability in the river basin is required to assure water security, and subsidize adaptative responses to extreme hydrological events.

1 Introduction

Climate oscillations can shift equilibrium states and cause the loss of stability of ecosystems and regional landscapes. The disturbance of shifting baseline influences biogeochemistry, biological productivity, biodiversity composition, and, ultimately, ecosystem services. The hydrological cycle is a critical biogeochemical process of a nested network of natural and social systems. Consequently, assuring water security for ecosystems, drinking water, economic development, and natural hazards is essential, particularly under persistent long term climate shifts further than discrete weather events. The resilience of socio-hydrological systems affected by climate oscillations at local and regional scales, and long-term changes at a global scale, have been compromised by intensive land use and land cover - LULC changes. LULC changes can amplify the frequency and intensity of climate extremes, resulting in highly severe environmental and socioeconomic impacts (Pan et al., 2015; Zhao et al., 2018; Gogoi et al., 2019). As a result, it has been recognized to assure that water security is crucial to achieving a better understanding of climate patterns and dynamics (Dore, 2005; Swaney et al., 2012).

The assessment of water availability and hydrological risks and hazards for sustainable water resources management must be based on sound information emphasizing spatial and temporal rainfall distribution in watersheds (Badr & Zaitchik, 2014; Shamir et al., 2015; Hartmann et al., 2016; Jepson et al., 2017; Vogel, 2017; Lima et al., 2018; Andreu et al., 2019; Gunda et al., 2019; Qin et al., 2019; Shikangalah & Mapani, 2019; Yang et al., 2019; Vera et al., 2020). Changes in rainfall patterns with extended dry periods reduce river discharge with effects on water supply, hydroelectricity production (Gohar & Cashman, 2016; Su et al., 2019), and disturbances on downstream ecosystems structure and functioning (Sabater et al., 2018).

River discharge reductions on lower sections of tropical and warm temperate coastal basins, under low and/or highly seasonal rainfall and fluvial discharge regulation, can lead to estuarine and groundwater salinization (Alber, 2002; Tweedley et al., 2019). Ecological effects can be related to disturbing nutrient dynamics, impairing feeding, mating and nesting habitats, and reducing the biodiversity of aquatic biological communities (Atrill & Power, 2000; Alber, 2002; Dai et al., 2006; Yin et al., 2014; Corbari et al., 2016; Costa et al., 2018; Lund-Hansen, 2018; Tweedley et al., 2019).

A concise understanding of climate dynamics requires the definition of standard indices for the assessment of climate data. In this respect, the World Meteorological Organization–WMO assembled 27 core indices of extreme climate in the RClimeDex software package for indices calculation and climate trends outputs (Zhang & Yang, 2004).

Geographic information systems (GIS) and geostatistical analysis have become powerful tools for rainfall spatial modeling and water resources management (Goovaerts, 1999; Mir et al., 2017; Passarella et al., 2020). GIS can handle analog, and digital georeferenced data spatially indexed in a database for problem-solving using spatial analysis. Geostatistical analysis has been considered as a practical approach for modeling climate variables due to high accuracy and low errors of spatial models. Experimental variograms allow the most suitable model fit for spatial data dependence, including directional effects (i.e., anisotropy) on regionalized variables, improving variable predictions and with low costs (Holdaway, 1996; Holawe & Dutter, 1999; Noori et al., 2014; Mendez & Calvo-Valverde, 2016; Ozturk & Kilic, 2016).

This study aims to analyze the spatial and temporal variability and trends of rainfall data using meteorological stations, from 1970 to 2017, at a coastal river basin in southeastern Brazil, Santa Maria da Vitória River Basin–SMVRB, to promote effective water resources management of the fluvial-estuarine hydrological system.

2 Materials and Methods

2.1 Study area

The Santa Maria da Vitória River Basin–SMVRB drains an area of 1,799.6 km^2 comprising the municipalities of Santa Maria de Jetibá, Santa Leopoldina and part of Cariacica, Serra, and Vitória in Espírito Santo state, southeastern Brazil (Figure 1a). The SMVRB drains to Vitória Bay estuarine system–VBES (42.9 km^2), which mangrove forests cover 57.9 % (24.8 km^2) of the area under a microtidal (<2.0 m) and semidiurnal regime. The VBES watershed (1,921 km^2), which embraces the other nine river basins, has a mean estimated discharge of 65.14 m^3/s (2.0×10^9 m^3/yr) with SMRVB contributing with 80% of fluvial discharge (Teubner Jr. et al., 2018).

The rugged SMVRB relief embraces elevations from sea level at Quaternary coastal plains, in the lower basin, to 1,421 m at the headwaters, where pre-Cambrian gneisses and

granitic rocks predominate. The average slope of SMVRB is 12.8%, with significant elevation changes in the middle basin section. The regional climate is seasonal, with a hot wet summer and dry, mild winter, with a mean annual rainfall of 1,300 mm (Teubner Jr. et al., 2018). Koppen climate classes are Cfb, Cfa, and Am and account to 42.3, 22.8, and 32.4 of the basin areas at the upper, middle, and lower sections, respectively (Alvares et al., 2013). The Aw class accounts for 2.5% of the SMVRB area within 200 and 400 m elevation in the middle basin section.

The SMVRB has three main water reservoirs, with two of them in operation for hydropower generation in the main river course: Rio Bonito (2.4 km^2 of surface area and 22.5 MW of hydropower capacity) with annual storage regulation; and Suiça (0.14 km^2 of surface area and 33.5 MW of hydropower capacity) with daily regulation (Teubner Jr. et al., 2018).

In 2012 the LULC of SMVRB was characterized by native Atlantic forest (45%) followed by pastureland (16%), croplands (14%), and Eucalyptus forestry (7%). Urban areas account for 4% of the river basin area and are primarily concentrated in the lower basin section (Figure 1c). In 2010, population counting for the whole VBES was 1,159,350 inhabitants, most of them living in the urban Great Vitória Metropolitan Area at the coastal plain. SMVRB is the primary source of water for urban supply (Teubner Jr. et al., 2018).

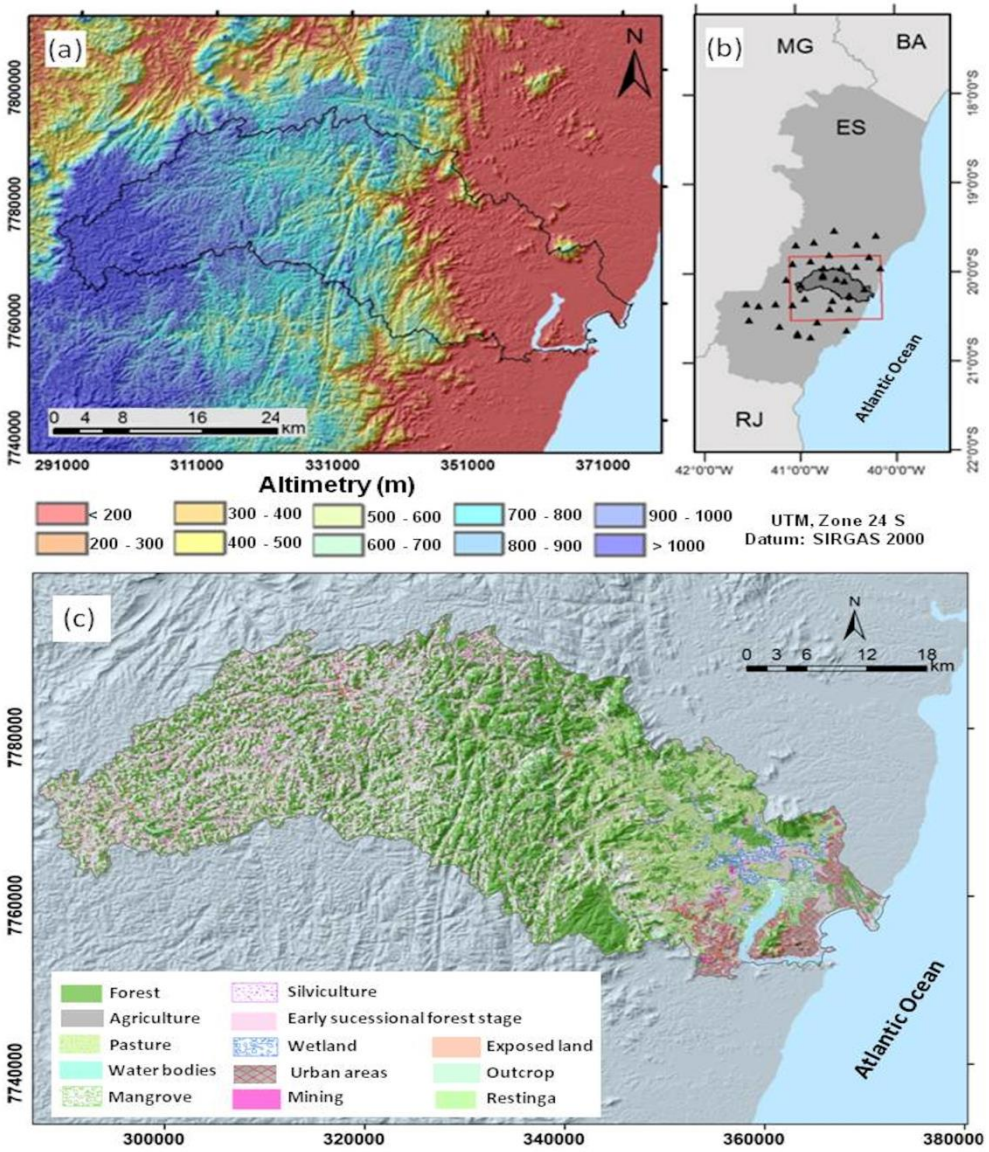

Figure 1. Study area: a) SMVRB digital elevation model; b) location of SMVRB and meteorological stations for rainfall data in the Espírito Sato State, Southeastern Brazil; c) 2012 land use and land cover–LULC (Restinga: coastal plain herbaceous and shrub vegetation), according to GEOBASES (2015).

2.2 Rainfall data

Rainfall data from 2004 to 2017 were obtained from 42 meteorological stations at Hidroweb, a database of hydrologic information of the National Water Agency (ANA) (Figure 1b). The dataset from 2018 to 2019 was not considered because of the incomplete records of several meteorological stations. When data gaps and inconsistencies were found in temporal series, gaps were filled, considering a threshold of 10% of monthly data. Multiple linear regressions considering a set of three meteorological stations, spatially nearer and within the same geomorphological feature, were applied as a filling method. Regressions with $r^2 > 0.7$ were considered, while months with lower coefficients were discarded from temporal series.

2.3 Interpolation of rainfall data and processing of continuous surface models

Continuous spatial distributions of rainfall data were interpolated for each month from 2004 to 2017. Geostatistical analysis with ordinary kriging with a spherical variogram model was applied to rainfall data using the GIS package ESRI ArcGIS 10.7 with UTM coordinate system and SIRGAS 2000 datum. As a statistical requirement for monthly means, outliers and non-normal distribution data (Naoum and Tsanis, 2004), assessed with the Shapiro-Wilk test and R software, were excluded. Rainfall predictions for the SMVRB were inferred with spatial correlations of meteorological station data through experimental variograms. As a geostatistical requirement, the spatial data structure analysis was based on the spatial correlation between samples and their distances (Goovaerts, 1999).

Interpolation results were evaluated considering reports of variograms parameters, cross-validation errors, linear regressions between predicted and measured values, rainfall prediction maps, and maps of associated errors. Adjustments on variograms parameters are required for high kriging capacity for climate datasets spatialization, including regions with low data densities (Campling et al., 2001; Aalto et al., 2012; Choudhury et al., 2015). Additionally, kriging procedures can consider, in variogram analysis, data anisotropy, which is a common feature of climate data (Holdaway, 1996).

Monthly mean rainfall models were developed with ESRI ArcGIS 10.7 raster algebra routines. Time series of annual rainfall for the same period, from 2004 to 2017, was computed considering annual precipitation. Descriptive statistics were acquired using ESRI ArcGIS 10.7 raster calculation routines for each continuous surface model of annual rainfall.

2.4 Climate Extreme Indices–CEI

The evaluation of climate change effects was computed using the software RClimDex with 11 rainfall related Climate Extreme Indices - CEI from the 27 core indices. The Expert Team proposed the RClimDex on Climate Change Detection Monitoring and Indices - ETCCDMI (Zhang & Yang, 2004) (Table 1). After the evaluation of discontinuities and gaps, a rainfall dataset of 34 meteorological stations, from 1970 to 2017, was selected for CEIs computation. Datasets with more than 25% of annual gaps and monthly datasets with more than three gaps were excluded. For each computed index, RClimDex provides as outputs statistical reports, linear trends based on least squares, statistical trend significance levels, according to the Fischer method, and standard error estimates (Zhang & Yang, 2004). In the present study, the confidence level for CEIs were 90 and 95%. Ordinary kriging with spherical models was applied to interpolate CEI data using ArcGIS.

Table 1

Selected indices of extreme climate applied in the study area

ID	Name	Definition	Unity
RX1day	1 day maximum rainfall	Maximum 1 day monthly rainfall	mm
RX5day	5 days maximum rainfall	Maximum 5 consecutive days monthly rainfall	mm
SDII	Simple daily index	The ratio of annual rainfall and rainy days (≥1 mm)	mm/day
R10mm	Days with intense rainfall	Days with rainfall ≥10 mm	days
R20mm	Days with high intense rainfall	Days with rainfall ≥ 20 mm	days
R50mm	Days with rainfall higher than 50 mm	Days with rainfall ≥ 50 mm	days
CDD	Consecutive days of droughts	Maximum consecutive days of rainfall < 1 mm	days
CWD	Consecutive rainfall days	Maximum consecutive days of rainfall ≥ 1 mm	days
R95p	Very wet days	Annual total PRCP when RR>95th percentile	mm
R99p	Extremely wet days	Annual total PRCP when RR>99th percentile	mm
PRCPTOT	Annual total wet day precipitation	Annual total PRCP in wet days (RR≥1mm)	mm

3 Results and Discussion

3.1 Rainfall temporal variability

The interpolation of monthly rainfall data, using spheric kriging, produced 168 continuous surface models with 30 m of spatial resolution and the associated cross-validation errors. Figures 2 show the mean monthly rainfall and related RMS. Lowest RMS were associated with lower data variability of dryer periods, principally after 2014. Seasonality of wet months (>120 mm) comprise from late spring to early fall, and dry months (<60 mm) from late fall to middle spring (Figure 2a and Table 2). December and November account for 35% of annual precipitation.

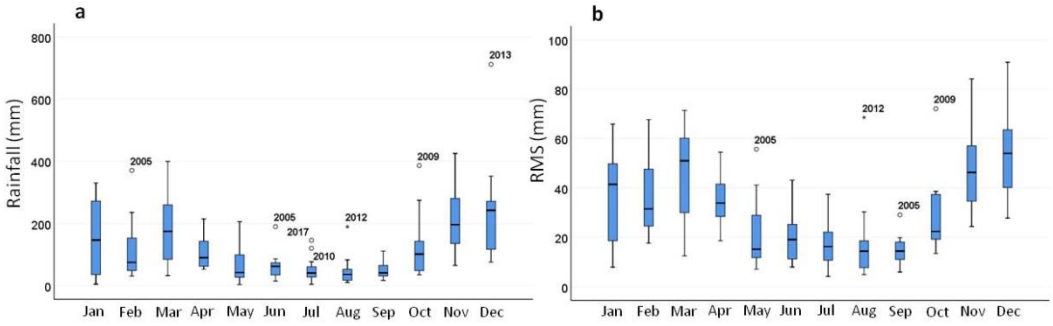

Figure 2. Boxplots of rainfall and estimated errors (RMS) in mm in the study area: a) mean monthly rainfall; b) mean RMS of monthly rainfall.

Table 2

Descriptive statistics of monthly rainfall (mm) for 2004 and 2017. Data from month rainfall spacial models

Month	Minimum	Maximum	Mean	Standard deviation
January	3.91	336.75	150.39	112.74
February	30.66	369.16	117.61	95.87
March	32.03	399.46	179.62	115.55
April	55.03	211.19	107.81	50.90
May	0.93	205.52	63.98	57.25
June	14.70	184.99	62.81	41.65
July	3.93	149.49	52.09	40.24
August	9.91	189.03	46.46	46.28
September	23.94	115.80	51.00	24.58
October	34.40	386.32	108.65	88.94
November	65.59	425.36	219.57	95.59
December	75.97	710.63	239.33	161.38

Mean annual rainfall along the 13 years was 1,339.4 ± 367.4 mm. 2005 and 2013 were the wettest years with 2,044.3 and 1,959.5 mm, respectively. For the Considering monthly averages from 2004 to 2017, the highest positive anomalies were concentrated in February, May, and June of 2005. The anomalous precipitation recorded for the year 2013 was concentrated in December, reaching three times the monthly average.

The driest years were 2015, 2007, and 2014, with 789.1, 928.0, and 949.8 mm of rainfall, respectively. However, the drought of 2014 and 2015 seems to be the most severe, considering the lower rainfall variability along the 14 years.

The highest rainfalls of November and December are related to the South Atlantic Convergence Zone (SACZ). SACZ is an important climatological feature of the austral summer in South America, with high precipitation extending NW to SE, from the Amazon toward southeastern Brazil, and occurring between October to March with a period of at least three days (Carvalho et al., 2004; Abrizzi & Ferraz, 2013). Conversely, the dry season, which extends from June to August, is primarily controlled by semi-permanent meteorological phenomena of South Atlantic, such as cold fronts (CF) and the South Atlantic Subtropical High (SASH) (Santos et al., 2019).

The anisotropic pattern of rainfall variograms indicates an NW trend for the wettest months. In contrast, for the dry season, the tendency is SW and S (Figure 3). Rainfall in the dry season is driven by the dominant CF and SASH atmospheric systems. During this season, the SASH is displaced from the middle South Atlantic Ocean towards the continent, where lower temperatures prevent low-pressure systems, decreasing rainfall (Santos et al., 2019).

Anisotropy is a parameter obtained by analyzing the structure of the data in the experimental variogram. It indicates a directional tendency of natural phenomena. Thus, the data show the best estimates of predictions with lower associated errors in a particular direction. Nevertheless, predictions of different anisotropic and isotropic variograms may not be significant (Haberlandt, 2007). Anisotropy is a common phenomenon associated to climate variables since its relation with other factors, whether climatic as preferential to wind direction, orogenic to geomorphology, geographic as the distance from the sea, among others (Arbia & Lfratta, 2002; Niemi et al., 2014; Wadoux et al., 2017).

The analysis of the experimental variograms of the mean monthly directional trends, for the period from 2004 to 2017, shows a relative homogenization of the anisotropy throughout the year (Figure 3). The mean annual anisotropy of rainfall in the study area, based on 168 monthly rainfall measurements, is oriented towards SW-S direction (133.7°) (Figure 3m). For the driest months, between June and August, the directional trend is oriented towards SW-S (Figure 3f-h). The wettest months, November and December, show preferential anisotropy towards NW. From January to April, anisotropy in the BHSMV is in the NE direction. From June to August, the direction follows S-SW.

The Espírito Santo central region is characterized by a marked change in elevation from NW to SE, from the hinterland towards the coast. This rouged relief influence the directional trends of rainfall anisotropy as a spatial dependent factor. A more refined understanding of rainfall anisotropy variability in the river basin would require a more spatially dense network of meteorological stations and extensive time series.

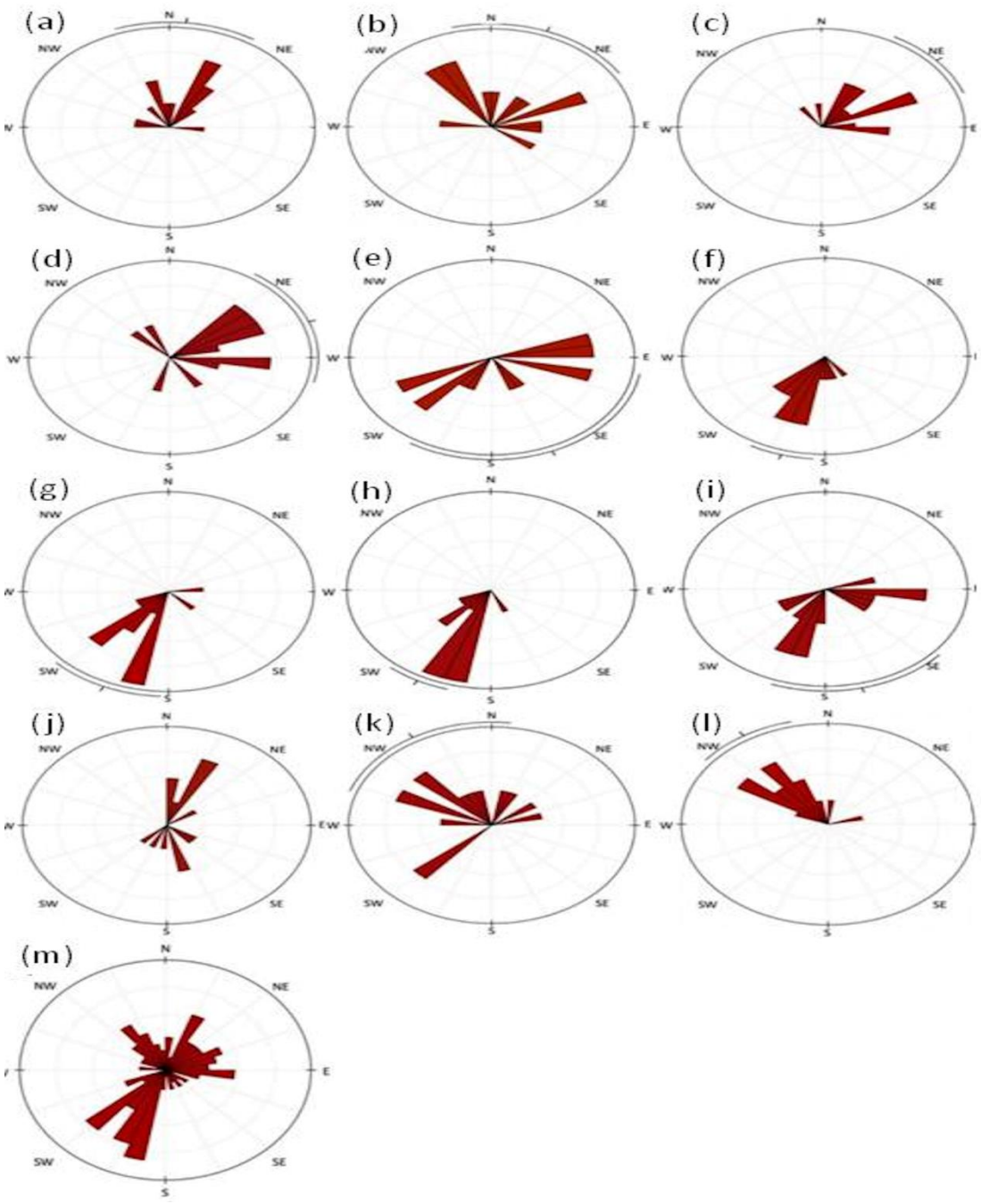

Figure 3. Variograms preferential directions of mean monthly (a-l) and annual rainfall (m) in the study area for the period of 2004 to 2017 (n = 168): a) January; b) February; c) March, d) April; e) May; f) June; g) July; h) August; i) September; j) October; k) November; l) December; (m) annual.

3.2 Rainfall spatial variability

Throughout the year, the spatial distribution of rainfall in the SMVRB is geographically heterogeneous, with lower precipitation in the upper and west basin sectors during the dry season. In the wettest month, December, the amount of rainfall is higher in the west part of the river basin. During December, the rainfall is related to the SACZ (Figure 3L; Figure 4L).

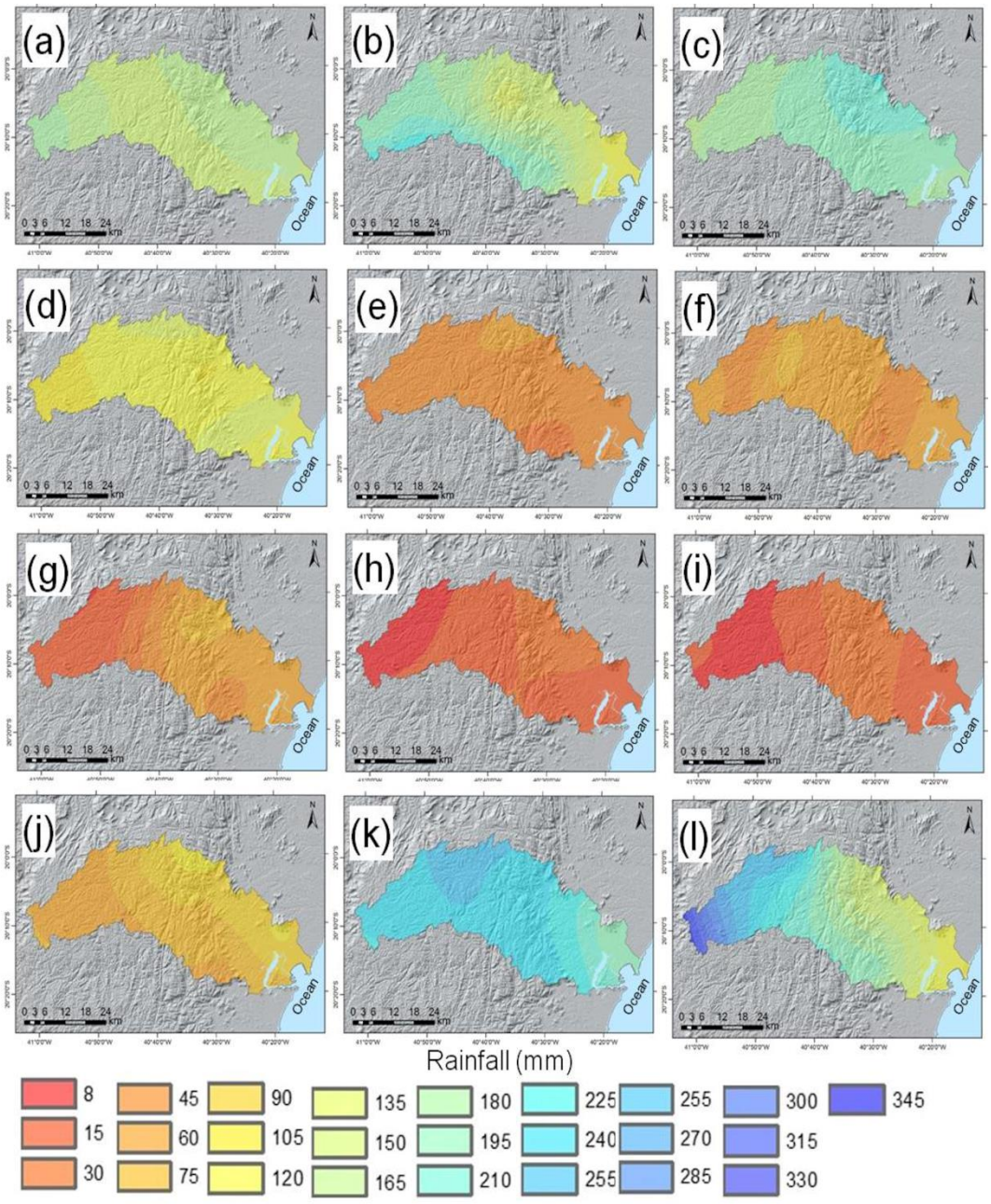

Figure 4. SMVRB mean monthly rainfall (mm) for the period of 2004 to 2017: a) January; b) February; c) March, d) April; e) May; f) June; g) July; h) August; i) September; j) October; k) November; l) December.

The spatial patterns of annual rainfall are shown in Figure 5. For the years 2005 and 2013, the wettest years, the precipitation was concentrated in the middle basin section, where the relief is more accentuated. The accumulation of rainfall in the middle section can also be observed in other years. This pattern demonstrates the influence of maritime and continentality on rainfall and associated regional instability lines.

In this sense, the distance from the ocean towards the continent, exert a wide range of influences on regional climate conditions. The hilly relief of the middle SMVRB, geomorphic, dominated the south Espírito Santo staggered levels. The foothills of mountain range concentrate and trap part of precipitation, producing a rain shadow with low rainfall towards the upper basin section where the Caparaó massive dominates. Therefore, the

mountain range increases precipitation associated with frontal rains at foothills of staggering levels. In the plateau, rainfall decreases toward the driest upper west part of the basin.

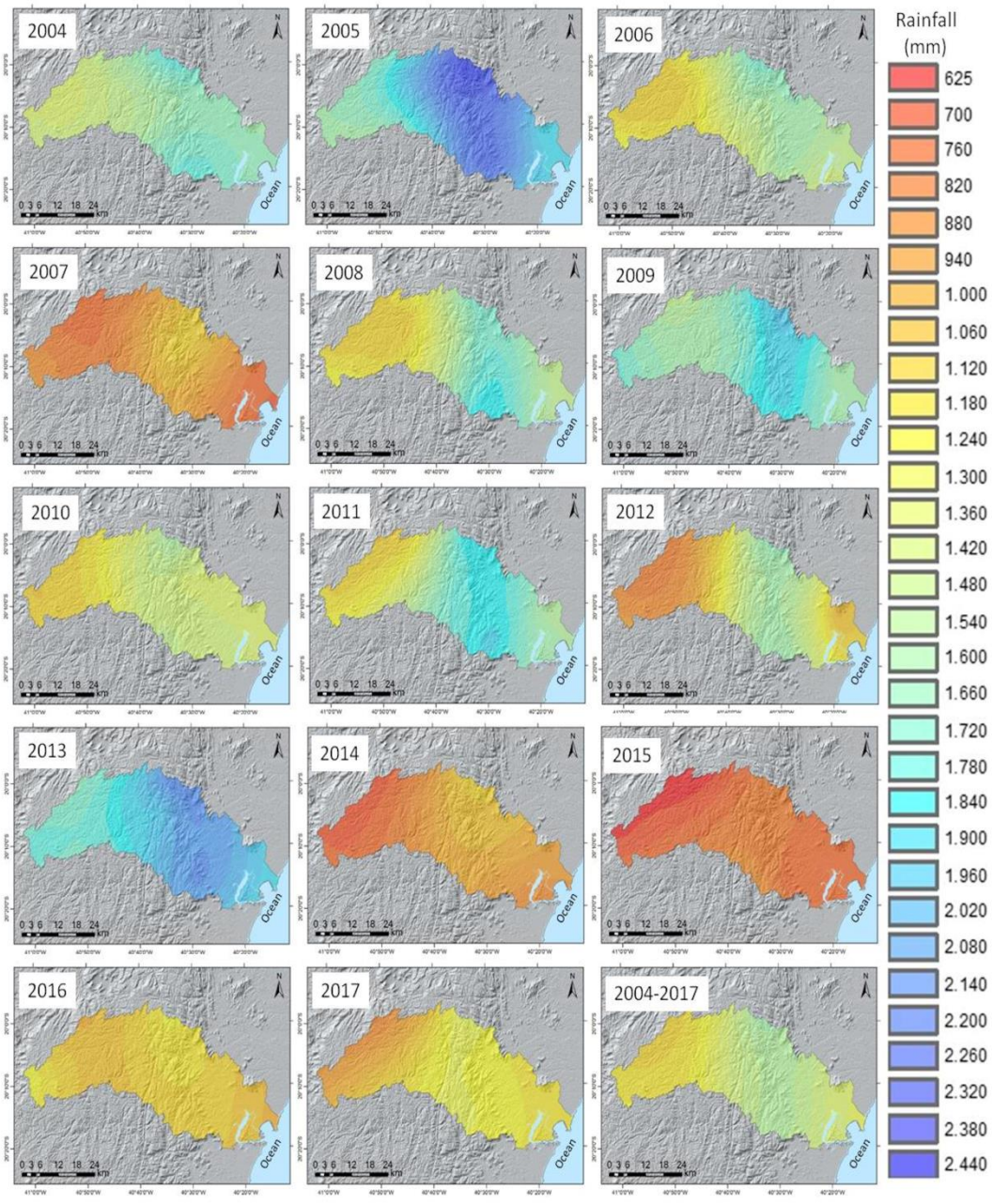

Figure 5. SMVRB annual rainfall (mm) for the period of 2004 to 2017.

3.3 Extreme Climate Indices

The analysis of time series trends is associated with its non-stationarity throughout its development to an average. Several factors that driven non-stationarity, are commonly related to factors inherent to the studied phenomenon, presenting as seasonal components, trend, or heterogeneity of variances (Milly et al., 2008; Milly et al., 2015). However, the non-stationarity of the data is a sophisticated statement that requires that the variable distribution depends on the time associated with a deterministic statistical function (Serinaldi & Kilsby, 2015; Serinaldi et al., 2018).

Climate indices have been commonly applied in the analysis of climate features, mainly for rainfall variables, due to the relevance of knowing the temporal distribution of rainfall for socioeconomic and environmental issues. Figure 6 shows the annual spatial features of CEI associated with rainfall at SMVRB.

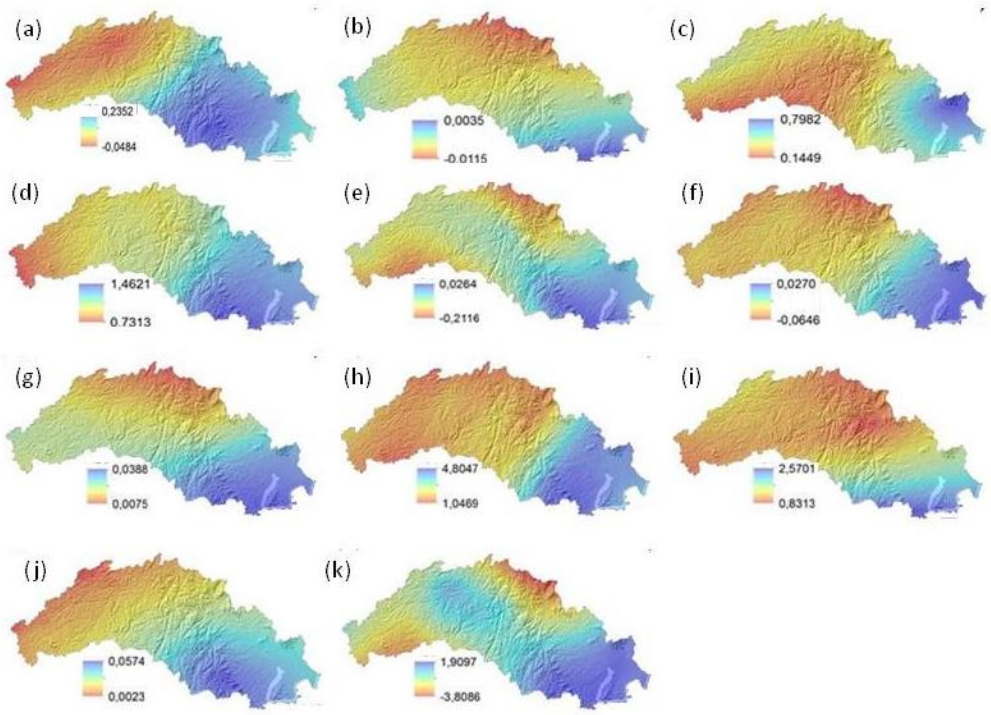

Figure 6. Rainfall indices at SMVRB computed with RClimDex from 1970 to 2017: a) CDD–consecutive dry days; b) CWD–consecutive wet days; c) RX1day–maximum rainfall amount in one day; d) RX5day–maximum rainfall amount in five days; e) RX10mm–number of days in a year with rainfall amount higher than 10 mm; f) RX20mm–number of days in a year with rainfall amount higher than 20 mm; g) RX50mm–number of days in a year with rainfall amount higher than 50 mm; h) R95p–extremely wet days with total annual higher than 95 percentiles; i) R99p–extremely wet days with total annual higher than 99 percentiles; j) SDII–simple day intensity index for rain; k) PRCPTOT–total annual rainfall.

The PRCPTOT index indicates that rainfall for rainy days (>1 mm) shows a negative trend for 71.4% meteorological stations. The PRCPTOT index shows a trend for rainfall below time-series average and drought conditions along half of the 60s, 80s, and 90s (Figure 7a). Spatial analysis of PRCPTOT presents a decrease towards W and NE, while towards E, in the coastal basin section, the amount of rainfall increase (Figure 6k). Overall, there is a trend for rainfall decrease in the upper basin sector, which is the contributing area with the complex runoff processes for water production in the basin. Moreover, the upper basin sector shows high water demands for crop irrigation, which could impair agriculture production and other economic activities if the negative trends of the PRCPTOT index are verified.

The analysis of consecutive dry days, computed with the CDD index, indicates a tendency of increase for a significant part of the basin, as shown for 82.3% climate stations, 37.9% of them with statistical significance. The trend of dryness is shown with the increase of the CDD index after 2014 (Figure 7b) and a sharp decrease of PRCPTOT (Figure 7a). The CDD index indicates a robust positive tendency for the lower basin section, with increasing rainfall intensity but concentrated in a few days (Figure 6a). The lower basin, particularly the coastal compartment, has been most urbanized, concentrates a significant part of the

population (Teubner Jr. et al., 2018), and is vulnerable to SACZ events of high rainfall with short duration. Urban impacts, such as flooding, landslides, and homeless inhabitants, have been reported in the Great Vitória after SACZ torrential rainfalls (Marchioro et al., 2016).

The statistical significance associated with high positive tendencies for the CWD index, which indicates consecutive wet days, were found for 14.7% of meteorological stations. A decreasing trend was evident in the temporal series (Figure 7c). The spatial trends of CWD for the coastal sector of SMVRB are following CDD and PRCCPTOP results (Figure 6b). Therefore, the tendency for increasing precipitation in a short time interval is indicated for the highly populated coastal sector. This trend increases the risks of flooding and impacts related to rainfall drainage (Marchioro et al., 2016).

The R10mm index shown a negative tendency in 85,3% stations, with 43.3% of them statistically significant. In general, the R10mm index follows previous indices' results with the tendency of rainfall reduction through the increase of consecutive dry days and concentrated rainfall in consecutive wet days in the lower section of the SMVRB. The R20mm index, which has shown negative trends, while the R50mm index is showing positive trends for 82.3% stations and a shift with increasing years with intensive rainfall (>50 mm) (Figure 6e-g and Figure 7d-e). Monthly or annual thresholds of rainfall indices are essential to identify different types of events throughout the historical series. This type of approach is commonly used in the climatological analysis to verify the frequency of days with extreme precipitation values.

The SDII has shown positive trends for daily rainfall intensity at 76.5% stations, with 30.8% of them with statistical significance, as shown in Figure 7f. Following the CDD and PRCPTOT indexes, SDII also shows a trend for high daily rainfall occurring in rare events in the coastal sector. Maximum daily rainfall rates are also in conformity to the coastal rainfall increase (Figure 6j).

The RX1day and RX5day indexes show positive trends for 76.5% climate stations, 34.6% of them with statistical significance, and 91.2% stations with 19,3% of them with statistical significance, respectively. These two indexes are following the other indexes analyzed with the trend of extended dry periods and short periods of intense rainfall, verified with more intensity in the eastern portion of SMVRB (Figure 6c-d).

For the long term, the R95p and R99p, which indicate extremely wet days, with total annual higher than 95 and 99 percentiles and positive trends for 85.3% and 76.5% climate stations, respectively, show a trend for high rainfall intensity in the short term, particularly in the coastal section. Trends of increasing very wet days and extremely wet days were evident in Figure 7g-h. The increasing rainfall on consecutive days, as indicated with the RX5day index, can lead to hydrological hazards in the coastal section.

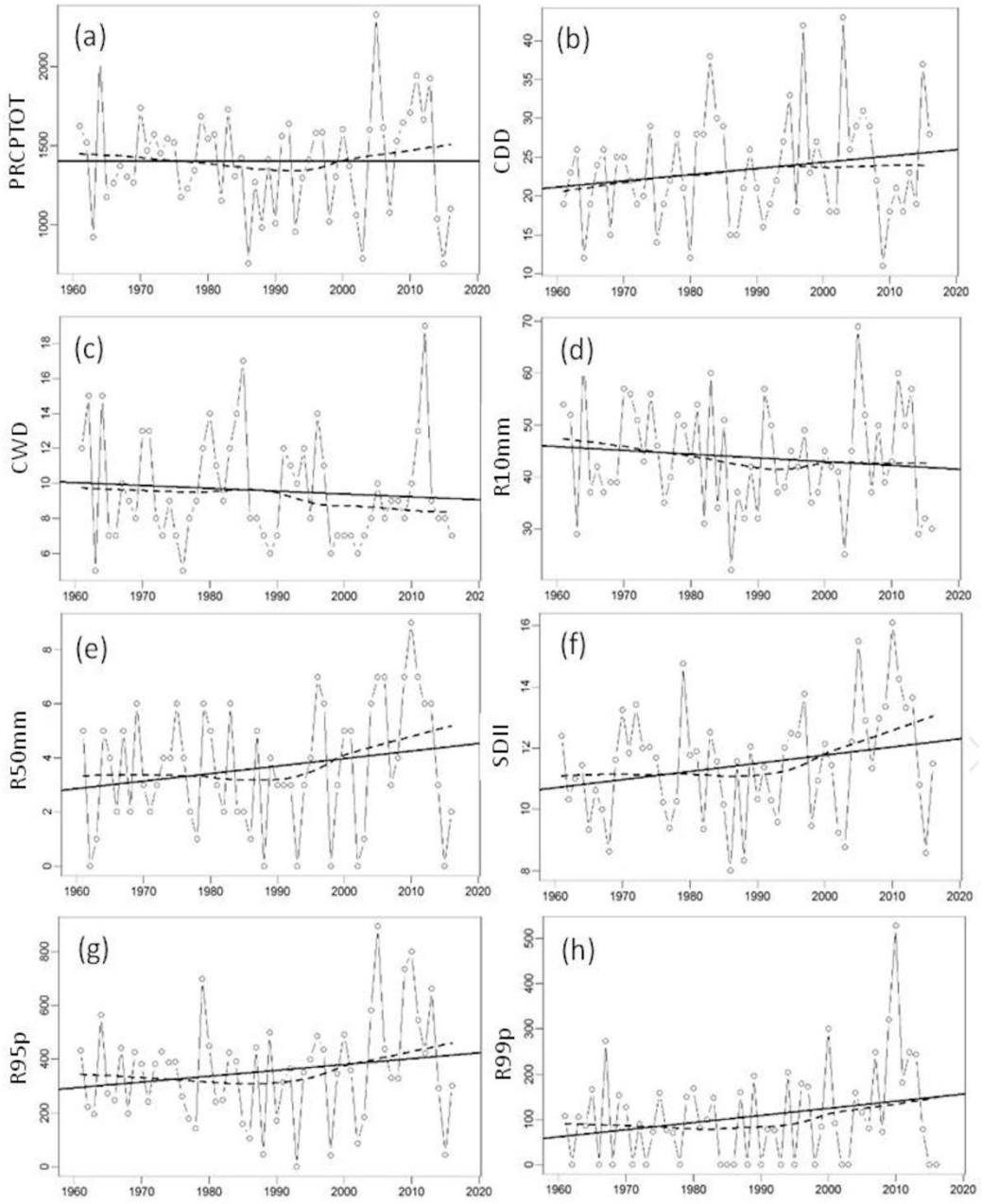

Figure 7. Linear trends of rainfall indices for Cachoeira Suíça a climate station for 1961 to 2017: a) PRCPTOT; b) CDD; c) CWD; d) R10mm; e) R50mm; f) SDII; g) R95p, and h) R99p. The continuous line is the linear regression trend, and the dashed line is the locally weighted scatterplot smoothing.

The consecutive droughts of the late 80s and early 90s can be associated to intense El Niño-Southern Oscillation (ENSO) events of 1987-1988, 1991-1992 and 1993-1994 (Sobral et al., 2019) and related positive anomalies of the sea surface temperature (SST) in the Tropical North Atlantic (Araújo & Brito, 2011). The ENSO is associated with changes in oceanic and atmospheric systems with the warming of Pacific Ocean SST affecting the climate system with the decrease of equatorial trade winds intensity and, consequently, the pattern of rainfall distribution in South America (Cane, 2005). As a cold phase of El Niño, La Niña (LN) is the cooling of Equatorial Pacific Ocean SST, decreasing rainfall in Southern South America. It is the extreme LN event of early 2007 and middle 2008 (Sobral et al., 2019).

Regardless of ENSO and LN interannual variability, the intensity and frequency of these climate oscillations have been increasing. This scenario can be aggravated with global warming of 1.5°C above the preindustrial levels as it has been predicted in several climate change models (Yeh, 2009; Cai et al., 2014; Wang et al., 2017).

Because of water scarcity scenarios, climate extreme indices based on precipitation have been applied to Brazilian arid and semiarid regions (Santos and Oliveira, 2017; Bezerra et al., 2018) and Southeastern region (Tafarello et al., 2016; Mohor & Mendiondo, 2017). Nevertheless, these indices are functional tools for analysis of positive trends of short-term intensive rainfall and, therefore, associated with hydrological hazards.

The climate extremes indices have indicated water scarcity at the SMVRB upper section, where agriculture and poultry activities are concentrated. The water shortage in the upper basin can also threaten the water regulation capacity of the Rio Bonito Reservoir (RBR), which regulates the fluvial discharge of River Santa Maria da Vitória and compromising the water supply of a part of Great Vitória metropolitan area. In September 2016, the water volume of RBR was below 30% of its storage capacity ($13.6\times10^{6}m^{3}$).

Thus, the understanding of rainfall characteristics and patterns can be an effective way to address water security and subsidize the formulation of public policies (Guzmam et al., 2017). The prediction of a 45% increase of irrigated cropland areas in Brazil for 2030 requires the best irrigation practices, improved reservoirs management, and adequate water resources grants to assure downstream water security (ANA, 2017). Water use grants issued by a public agency are a crucial tool for water resources regulation in Brazil. The granting system for water uses rights aims to assure river basin water security, through the analysis of quali and quantitative water availability.

Changes in rainfall patterns can lead to a reduction of river discharge and consequently, water scarcity in river basins impairing several economic activities (Marengo and Bernasconi, 2014; Escobar, 2015; Nobre et al., 2016). This scenario demands an evaluation of effective public policies and measures to ensure the storage of rainfall water in the fluvial system. Water storage can be achieved through construction and operation of reservoirs, and structural best management practices, such as small sediment basins (Strauch et al., 2013; Saad et al., 2018), as well as adopting more integrative approaches such as ecosystem-based management (Vörösmarty et al., 2018). In respect to the last issue, the payment for ecosystem services (PES) approaches recently adopted in Brazil, such as the Espirito Santo State Program for Increase of Forest Cover. The Reflorestar Program aims to restore the hydrological cycle through the restoration of forest cover in key river basin headwaters for water production with landowners' payment (SEAMA, 2019).

The integration of science and governance to foster public policies is complicated since the arrangement of several issues, including available technology and social behavior, and the lack of understanding of holistic approaches for implementing sustainable policies (Liu et al., 2015; Rose & Parsons, 2015; Mercure et al., 2016; Mercure et al., 2019). Understanding spatial and temporal rainfall distribution through spatial modeling is essential for the sustainable development of river basins.

4 Conclusions

Kriging was a practical approach to model rainfall data, through spatial interpolation, at SMVRB. The spatial analysis of rainfall datasets from 2004 to 2017 has shown the effect of basin geomorphology, with orographic retention of precipitation in the steep middle basin. Anisotropy of rainfall orientation was related to continental and regional climate processes.

Scenarios of water scarcity have been verified in recent years associated with climate events on a global scale. Rainfall-based extreme climate indices have shown a trend for high-intensity rains with short duration in the coastal section of SMVRB, which is located in the Great Vitória Metropolitan Area. Conversely, a tendency for rainfall reduction in the upper basin section may lead to a water shortage, which can be aggravated because of damming fluvial tributaries for intensive irrigation of croplands.

The spatial analysis and rainfall indices have shown the heterogeneity of distribution and trends of precipitation. We identify hotspots that need different approaches for water resources management. In upper section basin strategies for mitigating the drought associated with intensive agriculture is necessary. On the other hand, in the lower section, the trends for flooding in urban areas and the scarce water supply in some years show that it is essential to adopt adaptive measures to mitigate the socio-hydrological effects of changes on rainfall patterns. It is suggested that further studies emphasizing the extremes of climatic conditions must be carried out using a more extensive range of meteorological stations with statistical significance above 90%. Future studies using seasonal indices can also identify other patterns and trends not verified by the annual and monthly indices applied in the present work.

Develop the adoption of sustainability in public management of water resources should be in a participatory and decentralized scheme, involving diverse and representative stakeholders, integrating governance, science and society, presenting clear articulations between these spheres with the focus of rainfall distribution and water resources availability.

Acknowledgments

This study was financed in part by the Coordenação de Aperfeiçoamento de Pessoal de Nível Superior–Brasil (CAPES)–Finance Code 001. The research was stored in an institutional repository: <http://limnolab.ufes.br/data-repository>.

References

Aalto, J., Pirinen, P. & Heikkinen, J. (2012). Spatial interpolation of monthly climate data for Finland: comparing the performance of kriging and generalized additive models. *Theoretical and Applied Climatology, 112*, 99–111. https://doi.org/10.1007/s00704-012-0716-9

Alber, M.A. (2002). Conceptual model of estuarine freshwater inflow management. *Estuaries, 25*, 1246–1261. https://doi.org/10.1007/BF02692222

Alvares, C.A., Stape, J.L., Sentelhas, P.C., De Moraes, G., Leonardo, J. & Sparovek, G. (2013). Köppen's climate classification map for Brazil. *Meteorologische Zeitschrift, 22*(6), 711-728. https://doi.org/10.1127/0941-2948/2013/0507

Ambrizzi, T. & Ferraz, S.E.T. (2013). An objective criterion for determining the South Atlantic Convergence Zone. *Frontiers of Environmental Sciences, 17*, 1-9. https://doi.org/10.3389/fenvs.2015.00023

ANA–AGÊNCIA NACIONAL DAS ÁGUAS. (2017). *Atlas Irrigação: uso da água na agricultura irrigada*. Superintendência de Planejamento de Recursos Hídricos (SRH). Brasília–DF.

Andreu, A., Dube, T., Nieto, H., Mudau, A.E., González-Dugo, M., Guzinski, R. & Hülsmann, S. (2019). Remote sensing of water use and water stress in the African

savanna ecosystem at local scale–Development and validation of a monitoring tool. *Physics and Chemistry of the Earth, 112*, 154–164. https://doi.org/10.1016/j.pce.2019.02.004

Araújo, W.S & Brito, J.I.B. (2011). Indices of trends of climatic changes for the states of the Bahia and Sergipe by means of daily precipitacion indices and its relation with SST's of the Pacific and Atlantic. *Revista Brasileira de Meteorologia, 26* (4), 541- 554. . https://doi.org/10.1590/S0102-77862011000400004

Arbia, G. & Lafratta, G. (2002). Anisotropic spatial sampling designs for urban pollution. *Applied Statistics. 51*(2), 223–234. https://doi.org/0035–9254/02/51223

Atrill, M.J. & Power, M. (2000). Modelling the effect of drought on estuarine water quality. *Water Research, 34*(5),1584-1594. https://doi.org/10.1016/S0043-1354(99)00305-X

Badr, H.S. & Zaitchik, B.F. (2014). Application of Statistical Models to the Prediction of Seasonal Rainfall Anomalies over the Sahel. *Journal of Applied Meteorology And Climatology*, *53*(3), 614–636. 2014. https://doi.org/10.1175/JAMC-D-13-0181.1

Bezerra, B.G., Silva, L.L., Silva, C.M.S. & Carvalho, G.G. (2018). Changes of precipitation extremes indices in São Francisco River Basin, Brazil from 1947 to 2012. *Theoretical and Applied Climatology, 135*, 565–576. https://doi.org/10.1007/s00704-018-2396-6

Cai, W., Borlace, S., Lengaigne, M., Rensch, P., Collins, M., Vecchi, G., Timmermann, A., Santoso, A., Mcphaden, M.J., Wu, L., England, M.H., Wang, G., Guilyardi, E. & Jin, F.-F. (2014). Increasing frequency of extreme El Niño events due to greenhouse warming. *Nature Climate Change, 4*, 111–116. https://doi.org/10.1038/NCLIMATE2100

Campling, P., Gobin, A. & Feyen, J. (2001). Temporal and spatial rainfall analysis across a humid tropical catchment. *Hydrological Process, 15*, 359-375. https://doi.org/10.1002/hyp.98

Cane, M.A. (2005). The evolution of El Niño, past and future. *Earth and Planetary Science Letters, 230*, 227–240. https://doi.org/10.1016/j.epsl.2004.12.003

Carvalho, L.M.V., Jones, C. & Liebmann, B. (2004). The South Atlantic Convergence Zone: intensity, form, persistence, and relationships with iIntraseasonal to interannual activity and extreme rainfall. *Journal of Climate, 17*, 88-108. https://doi.org/10.1175/1520-0442(2004)017<0088:TSACZI>2.0.CO;2

Choudhury, N. H., Rahman, A. & Ferdousi, S. (2015). Kriging Infill of Missing Data and Temporal Analysis of Rainfall in North Central Region of Bangladesh. *Journal of Climatology & Weather Forecasting, 3*(3). https://doi.org/10.4172/2332-2594.1000141

Corbari, C., Lassini, F. & Mancini, M. (2016). Effect of intense short rainfall events on coastal water quality parameters from remote sensing data. *Continental Shelf Research, 123*, 18–28. https://doi.org/10.1016/j.csr.2016.04.009

Costa, C.R., Costa, M.F., Dantas, D.V. & Barletta, M. (2018). Interannual and seasonal variations in estuarine water quality. *Frontiers in Marine Science, 5*, 301 https://doi.org/10.3389/fmars.2018.00301

Dai, M., Guo, X., Zhai, W., Yuan, L., Wang, B., Wang, L., Cai, P., Tang, T. & Cai, W. J. (2006). Oxygen depletion in the upper reach of the Pearl River estuary during a winter

drought. *Marine Chemistry, 102*, 159–169. https://doi.org/10.1016/j.marchem.2005.09.020

Dore, M.H.I. (2005). Climate change and changes in global precipitation patterns: What do we know? *Environment International, 31*, 1167-1181. https://doi.org/10.1016/j.envint.2005.03.004

Escobar, H. (2015). Water security. Drought triggers alarms in Brazil's biggest metropolis. *Science, 347*(6224), 812. https://doi.org/10.1126/science.347.6224.812

GEOBASES, Mapeamento 2012–2015–Uso e cobertura do solo. Available in https://geobases.es.gov.br/links-para-mapes1215

Gogoi, P. P., Vinoj, V., Swain, D, Dash, J. & Tripathy, S. (2019). Land use and land cover change effect on surface temperature over Eastern India. *Scientific Reports* 9, 8859 https://doi.org/10.1038/s41598-019-45213-z

Gohar, A.A. & Cashman, A. (2016). A methodology to assess the impact of climate variability and change on water resources, food security and economic welfare. *Agricultural Systems, 147*, 51-64. http://dx.doi.org/10.1016/j.agsy.2016.05.008 0308-521X

Goovaerts, P. (1999). Using elevation to aid the geostatistical mapping of rainfall erosivity, *Catena, 34*, 227-242. https://doi.org/10.1016/S0341-8162(98)00116-7.

Gunda, T., Hess, D., Hornberger, G. M. & Worland, S. (2019). Water security in practice: The quantity-quality-society nexus. Water Security, 6:100022. https://doi.org/10.1016/j.wasec.2018.100022

Guzmán, D.A., Mohor, G.S., Taffarello, D. & Mendiondo, E.M. (2017). Economic impacts of drought risks for water utilities through Severity-Duration-Frequency framework under climate change scenarios. *Hydrology and Earth System Sciences Discuss*., https://doi.org/10.5194/hess-2017-615

Haberlandt, U. (2007). Geostatistical interpolation of hourly precipitation from rain gauges and radar for a large-scale extreme rainfall event. *Journal of Hydrology, 332*, 144–157. https://doi.org/10.1016/j.jhydrol.2006.06.028

Hartmann, H., Snow, J., Su, B. & Jiang, T. (2016). Seasonal predictions of precipitation in the Aksu-Tarim River basin for improved water resources management. *Global and Planetary Change, 147*, 86–96. https://doi.org/10.1016/j.gloplacha.2016.10.018

Holawe, F. & Dutter, R. (1999). Geostatistical study of precipitation series in Austria: time and space. *Journal of Hydrology, 219*, 70–82. https://doi.org/10.1590/0001-3765201620150103

Holdaway, M.R. (1996). Spatial modeling and interpolation of monthly temperature using kriging. *Climate Research, 6*, 215-225. https://www.jstor.org/stable/24864559

Jepson, W., Budds, J., Eichelberger, L., Harris, L., Norman, E., O'reilly, K., Pearson, A., Shah, S., Shinn, J., Staddon, C., Stoler, J., Wutich, A. & Young, S. (2017). Advancing human capabilities for water security: A relational approach. *Water Security, 1*, 46-52.. https://doi.org/10.1016/j.wasec.2017.07.001

Lima G. N., Lombardo, M. A. & Magaña, V. (2018). Urban water supply and the changes in the precipitation patterns in the metropolitan area of São Paulo–Brazil. *Applied Geography, 9*, 223–229. https://doi.org/10.1016/j.apgeog.2018.03.010

Liu, J., Mooney, H., Hull, V., Davis, S. J., Gaskell, J., Hertel, T., Lubechenco, J., Seto, K. C., Gleick, P., Kremen, C. & Li, S. (2015). Systems integration for global sustainability. *Science, 347*(6225), 1.258.832. https://doi.org/10.1126 /science.1258832

Lund-Hansen, L.C., Jensen, K.T., Andersen, T.J., Nielsen, M.H., Doan-Nhu, H. & Nguyen-Ngoc, L. (2018). Impacts and effects of a historical high and ENSO linked freshwater inflow in the tropical estuary Nha Phu, southeast Vietnam. *Regional Studies in Marine Science, 17*, 28–37. https://doi.org/10.1016/j.rsma.2017.11.012

Marchioro, E., Silva, G.M. & Correa, W.S.C. (2016). A zona de convergência do Atlântico sul e a precipitação pluvial do município de Vila Velha (ES): repercussões sobre as inundações. *Revista do Departamento de Geografia, 31*, 101-117. http://dx.doi.org/10.11606/rdg.v31i0.108447

Marengo, J.A. & Bernasconi, M. (2014). Regional differences in aridity/drought conditions over Northeast Brazil: present state and future projections. *Climatic Change, 129*, 103-115. http://dx.doi.org/10.1007/s10584-014-1310-1

Mendez, M. & Calvo-Valverde, L. (2016). Assessing the performance of several rainfall interpolation methods as evaluated by a conceptual hydrological model. *Procedia Engineering, 154*, 1050-1057. https://doi.org/10.1016/j.proeng.2016.07.595

Mercure, J.-F., Pollitt, H., Bassi, A.M., Viñuales, J. E. & Edwards, N.R. (2016). Modelling complex systems of heterogeneous agents to better design sustainability transitions policy. *Global Environmental Change, 37*, 102–115. http://dx.doi.org/10.1016/j.gloenvcha.2016.02.003

Mercure, J.-F., Paim, M.A., Bocquillon, P., Lindner, S., Salas, P., Martinelli, P., Berchin, I.I., Andrade Guerra, J.B.S.O., Derani, C., Albuquerque Junior, C.L., Ribeiro, J.M.P., Knobloch, F., Pollitt, H., Edwards, N.R., Holden, P.B., Foley, A., Schaphoff, S., Faraco, R.A. & Vinuales, J.E. (2019). System complexity and policy integration challenges: The Brazilian Energy-Water-Food Nexus. *Renewable and Sustainable Energy Reviews, 105*, 230–243. https://doi.org/10.1016/j.rser.2019.01.045

Milly, P.C D., Betancourt, J., Falkenmark, M., Hirsch, R.M., Kundzewics, Z.W., Lettenmaier, D. P. & Stouffer, R. (2008). Stationarity is dead: Whither water management? *Climate Change, 139*, 573–574. https://doi.org/10.1126 /science.1151915

Milly, P.D.C., Betancourt, J., Falkenmark, M., Hirsch, R.M., Kundzewics, Z.W., Lettenmaier, D. P., Stouffer, R. Dettinger, M.D. & Krysanova, V. (2015). On Critiques of ‘‘Stationarity is dead: whither water management?’ *Water Resources Research, 51*(9), 7785-7789. https://doi.org/10.1002/2015WR017408

Mir, A., Piri, J. & Kisi, O. (2017). Spatial monitoring and zoning water quality of Sistan River in the wet and dry years using GIS and geostatistics. *Computers and Electronics in Agriculture, 135*, 38–50. http://dx.doi.org/10.1016/j.compag.2017.01.022

Mohor, G.S. & Mendiondo, E.M. (2017). Economic indicators of hydrologic drought insurance under water demand and climate change scenarios in a Brazilian context. *Ecological Economics, 140*, 66–78. https://doi.org/10.1016/j.ecolecon.2017.04.014

Naoum, S. & Tsanis, I.K. (2004). Ranking spatial interpolation techniques using a GIS-based DSS. *Global Nest Jornal, 6*(1), 1-20. https://doi.org/10.30955/gnj.000224

554 Niemi, T.J., Kokkonem, T. & Seed, A.W. (2014). A simple and effective method for
555 quantifying spatial anisotropy of time series of precipitation fields. *Water Resources*
556 *Research, 50* (7), 5906-5925. https://doi.org/10.1002/2013WR015190

557 Nobre, C.A., Marengo, J.A., Seluchi, M.E., Cuartas, L.A. & Alves, L.M. (2016). Some
558 characteristics and impacts of the drought and water crisis in Southeastern Brazil
559 during 2014 and 2015. *Journal of Water Resource and Protection, 8*(2), 252-262.
560 https://doi.org/10.4236/jwarp.2016.82022

561 Noori, M.J., Hassan, H.H. & Mustafa, Y.T. (2014). spatial estimation of rainfall distribution
562 and its classification in Duhok Governorate using GIS. *Journal of Water Resource*
563 *and Protection, 6*, 75-82. http://dxdoi.org/10.4236/jwarp.2014.62012

564 Ozturk, D. & Kilic, F. (2016). Geostatistical approach for spatial interpolation of
565 meteorological data. *Anais da Academia Brasileira de Ciências 88*(4), 2121-2136.
566 http://dx.doi.org/10.1590/0001-3765201620150103

567 Pan T., Wu S. & Liu, Y. (2015). Relative Contributions of Land Use and Climate Change to
568 Water Supply Variations over Yellow River Source Area in Tibetan Plateau during
569 the Past Three Decades. *PLoS ONE, 10*(4), e0123793.
570 http://dx.doi.org/10.1371/journal.pone.0123793

571 Passarella, G., Bruno, D., Lay-Ekuakille, A., Maggi S., Masciale, R. & Zaccaria, D. (2020).
572 Spatial and temporal classification of coastal regions using bioclimatic indices in a
573 Mediterranean environment. *Science of the Total Environment, 700*, 134415.
574 https://doi.org/10.1016/j.scitotenv.2019.134415

575 Qin, K., Liu, J., Yan, L. & Huang, H. (2019). Integrating ecosystem services flows into water
576 security simulations in water scarce areas: Present and future. *Science of the Total*
577 *Environment 670,* 1037–1048. https://doi.org/10.1016/j.scitotenv.2019.03.263 0048-
578 9697

579 Rose, N. A. & Parsons, E. C. M. (2015). "Back off, man, I'm a scientist!": When marine
580 conservation science meets policy. *Ocean & Coastal Management, 115*, 71-76.
581 https://doi.org/10.1016/j.ocecoaman.2015.04.016

582 Saad, S.I., Mota da Silva, J., Silva, M.L.N., Guimarães, J.L.B., Sousa Júnior, W.C.,
583 Figueiredo, R.D.O. & Rocha, H.R. (2018). Analyzing ecological restoration strategies
584 for water and soil conservation. *PLoS ONE, 13*(2), e0192325.
585 https://doi.org/10.1371/journal.pone.0192325

586 Sabater, S., Bregoli, F., Acuña, V., Barceló, D., Elosegi, A., Ginebreda, A., Marcé, R.,
587 Muñoz, I., Sabater-Liesa, L. & Ferreira, V. (2018). Effects of human-driven water
588 stress on river ecosystems: a meta-analysis. *Scientific Reports, 8*, 11462.
589 https://doi.org/10.1038/s41598-018-29807-7

590 Santos, V., Gastmans, D., Sánchez-Murillo, R., Gozzo, L. F., Batista, L. V., Manzione, R.L.
591 & Martinez, J. (2019). Regional atmospheric dynamics govern interannual and
592 seasonal stable isotope composition in southeastern Brazil. *Journal of Hydrology,*
593 *579*, 124136. https://doi.org/10.1016/j.jhydrol.2019.124136

594 Santos, C.A.C. & Oliveira, V.G. (2017). Trends in extreme climate indices for Pará State,
595 Brazil. *Revista Brasileira de Meteorologia, 32(*1), 13-24.
596 http://dx.doi.org/10.1590/0102-778632120150053

SEAMA–Secretaria de Estado do Meio Ambiente e Recursos Hídricos. *Diário Oficial dos Poderes do Estado: Portaria Nº 005-R, de 22 de março de 2019*. Available in https://seama.es.gov.br/o_que_e_reflorestar Access in Jan 2020.

Serinaldi, F. & Kilsby, C.G. (2015). Stationarity is undead: uncertainty dominates the distribution of extremes. *Advances in Water Resources, 77*, 17-36. http://dx.doi.org/10.1016/j.advwatres.2014.12.013

Serinaldi, F., Kilsby, C.G. & Lombardo, F. (2018). Untenable nonstationarity: an assessment of the fitness for purpose of trend tests in hydrology. *Advances in Water Resources, 111*, 132-155. http://dx.doi.org/10.1016/j.advwatres.2017.10.015

Shamir, E., Megdal, S.B., Carillo, C., Castro, C.L., Chang, H.I., Chief, K., Corkhill, F. E., Eden, S., Georgakakos, K. P., Nelson, K. M. & Prietto, J. (2015). Climate change and water resources management in the Upper Santa Cruz River, Arizona. *Journal of Hydrology, 521*, 18-33. http://dx.doi.org/10.1016/j.jhydrol.2014.11.062

Shikangalah, R.N. & Mapani, B. (2019). Precipitation variations and shifts over time: Implication on Windhoek city water supply. *Physics and Chemistry of the Earth, 112*, 103–112. https://doi.org/10.1016/j.pce.2019.03.005

Sobral, B. S., Oliveira-Júnior, J. F., Gois, G., Pereira-Júnior, E. R., Terassi, P. M. B., Muniz-Júnior, G. R., Lyra, G. B. & Zeri, M. (2019). Drought characterization for the state of Rio de Janeiro based on the annual SPI index: trends, statistical tests and its relation with ENSO. *Atmospheric Research, 220*, 141–154. https://doi.org/10.1016/j.atmosres.2019.01.003

Strauch, M., Lima, J. E. F. W., Volk, M., Lorz, C. & Makeschin, F. (2013). The impact of Best Management Practices on simulated streamflow and sediment load in a Central Brazilian catchment. *Journal of Environmental Management, 127*, S24-S36. http://dx.doi.org/10.1016/j.jenvman.2013.01.014

Su, Y., Gao, W. & Guan, D. (2019). Integrated assessment and scenarios simulation of water security system in Japan. *Science of the Total Environment, 671*, 1269–1281. https://doi.org/10.1016/j.scitotenv.2019.03.373 0048-9697

Swaney, D. P., Humborg, C., Emeis, K., Kannen, A., Silvert, W., Tett, P., Pastres, R., Solidoro, C., Yamamuro, M., Hénocque, Y. & Nicholls, R. (2012). Five sale questions of scale for the coastal zone. *Estuarine, Coastal and Shelf Science, 96*, 9-21. https://doi.org/10.1016/j.ecss.2011.04.010

Taffarello, D., Mohor, G.S., Calijuri, M.C. & Mendiondo, E.M. (2016). Field investigations of the 2013–14 drought through quali-quantitative freshwater monitoring at the headwaters of the Cantareira System, Brazil. *Water International, 41*(5), 776-800. http://dx.doi.org/10.1080/02508060.2016.1188352

Teubner Jr., F. J., Lima, A. T. M. & Barroso, G. F. (2018). Emission rates of nitrogen and phosphorus in a tropical coastal river basin: a strategic management approach. *Environmental Monitoring and Assessment, 190*, 747 https://doi.org/10.1007/s10661-018-7101-9

Tweedley, J. R., Dittmann, S. R., Whitfield, A. K., Withers, K., Hoeksema, S. D. & Potter, I. C. (2019). *Hypersalinity: Global distribution, causes, and present and future effects on the biota of estuaries and lagoons*. Wolanski, E., Day, J. W., Elliott, M. & Ramachandran, R. Coasts and estuaries: the future, Elsevier, 523-546. https://doi.org/10.1016/B978-0-12-814003-1.00030-7

642 Vera, J F.R., Mera, Y.E.Z. & Pérez-Martín, M.A. (2020). Adapting water resources systems
643 to climate change in tropical areas: Ecuadorian coast. *Science of the Total*
644 *Environment. 703*, 135554. https://doi.org/10.1016/j.scitotenv.2019.135554

645 Vogel, R. M. (2017). Stochastic watershed models for hydrologic risk management. *Water*
646 *Security, 1*, 28-35. 2017. https://doi.org/10.1016/j.wasec.2017.06.001.

647 Vörösmarty, C. J., Osuna, V. R., Cak, A. D., Bhaduri, A., Bunn, S. E., Corsi, F.,
648 Gastelumendi, J., Green, P., Harrison, I., Lawford, R., Marcotullio, P. J., McClain,
649 M., McDonald, R., McIntyre, P., Palmero, M., Robarts, R. D., Szöllösi-Nagy, A.,
650 Tessler, Z. & Uhlenbrook, S. (2018). Ecosystem-based water security and the
651 Sustainable Development Goals (SDGs). *Ecohydrology & Hydrobiology, 18*(4), 317-
652 333. https://doi.org/10.1016/j.ecohyd.2018.07.004

653 Wadoux, A.M.J-C, Brus, DJ., Rico-Ramirez, M.A. & Heuvelink, G.B.M. (2017). Sampling
654 design optimization for rainfall prediction using a non-stationary geostatistical model.
655 *Advances in Water Resources, 107*, 126–138.
656 https://doi.org/10.1016/j.advwatres.2017.06.005

657 Wang, G., Gan, B., Cai, W. & Wu. L. (2017). Continued increase of extreme El Niño
658 frequency long after 1.5°C warming stabilization. *Natural Climate Change, 7*, 568-
659 573. https://doi.org/10.1038/NCLIMATE3351

660 Yang, H., Xiao, H., Guo, C. & Sun, Y. (2019). Spatial-temporal analysis of precipitation
661 variability in Qinghai Province, China. *Atmospheric Research, 228*, 242–260.
662 https://doi.org/10.1016/j.atmosres.2019.06.005

663 Yeh, S.W, Kug, J. S. Dewite, B., Kwon, M. H., Kirtman, B.P. & Jin, F.F. (2009). El Niño in a
664 changing climate. *Nature 461*, 511-515. https://doi.org/10.1038/nature08316

665 Yin, K., Lin, Z. & Ke, Z. (2004). Temporal and spatial distribution of dissolved oxygen in the
666 Pearl River Estuary and adjacent coastal waters. *Continental Shelf Rearch, 24*, 1935-
667 1948. https://doi.org/10.1016/j.csr.2004.06.017

668 Zhang, X. & Yang, F. (2004). *RClimDex (1.0) user manual*. Environment Canada, 23pp.
669 [available at: http://etccdi.pacificclimate.org/RClimDex/RClimDexUserManual.doc]

670 Zhao, Z., Liu, G., Liu, Q., Huang, C. & Li, H. (2018). Studies on the spatiotemporal
671 variability of river water quality and its relationships with soil and precipitation: a
672 case study of the Mun river basin in Thailand. *International Journal of Environmental*
673 *Research and Public Health, 15*, 2466. https://doi.org/10.3390/ijerph15112466

Figure 1.

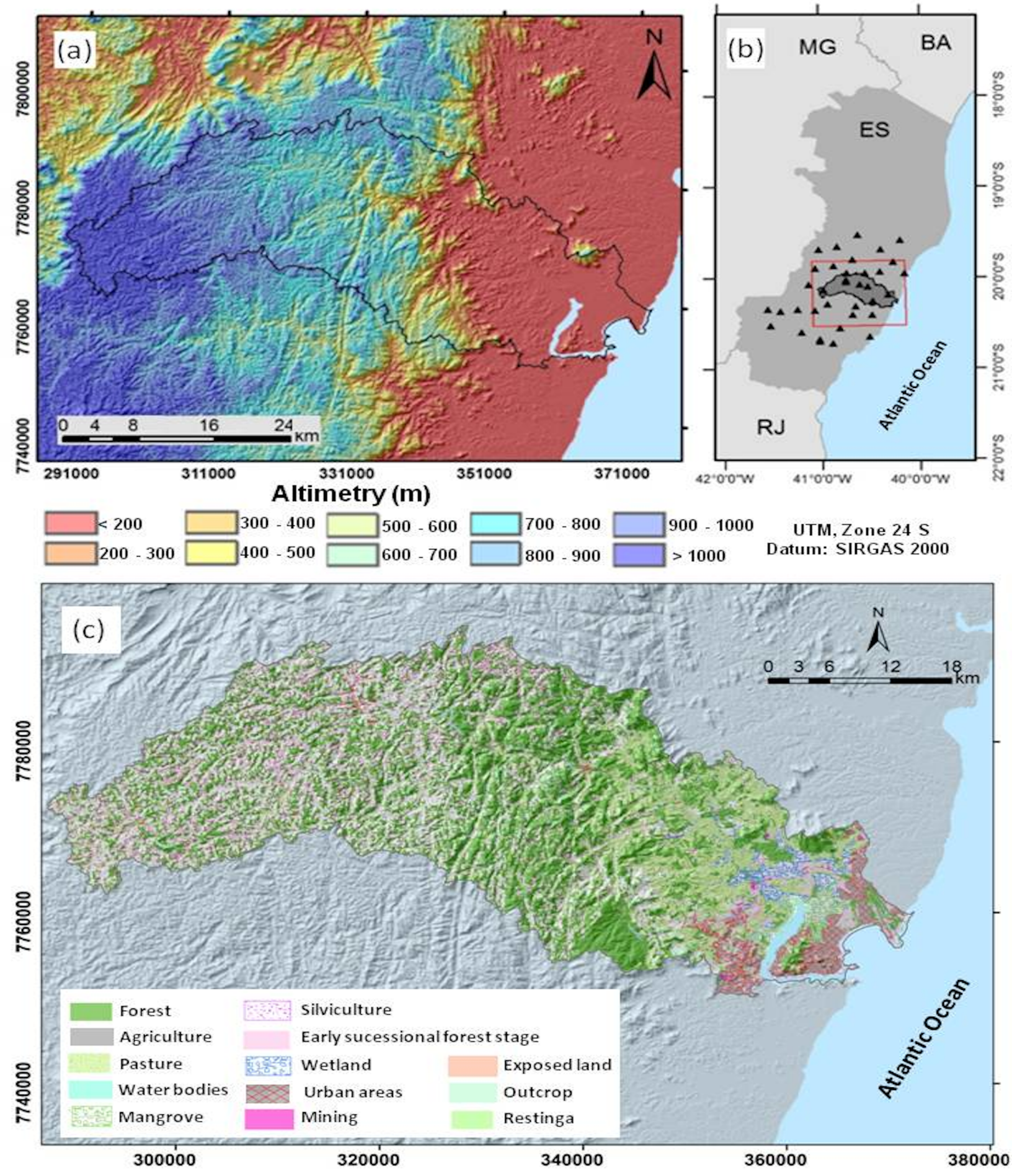
(a)
N
0 4 8 16 24 km
7800000
7780000
7760000
7740000
291000
311000
331000
351000
371000
(b)
MG
BA
ES
RJ
Atlantic Ocean
18°0'0"S
19°0'0"S
20°0'0"S
21°0'0"S
22°0'0"S
42°0'0"W
41°0'0"W
40°0'0"W
Altimetry (m)
< 200
200 - 300
300 - 400
400 - 500
500 - 600
600 - 700
700 - 800
800 - 900
900 - 1000
> 1000
UTM, Zone 24 S
Datum: SIRGAS 2000
(c)
N
0 3 6 12 18 km
Forest
Agriculture
Pasture
Water bodies
Mangrove
Silviculture
Early sucessional forest stage
Wetland
Urban areas
Mining
Exposed land
Outcrop
Restinga
Atlantic Ocean
7780000
7760000
7740000
300000
320000
340000
360000
380000

Figure 2.

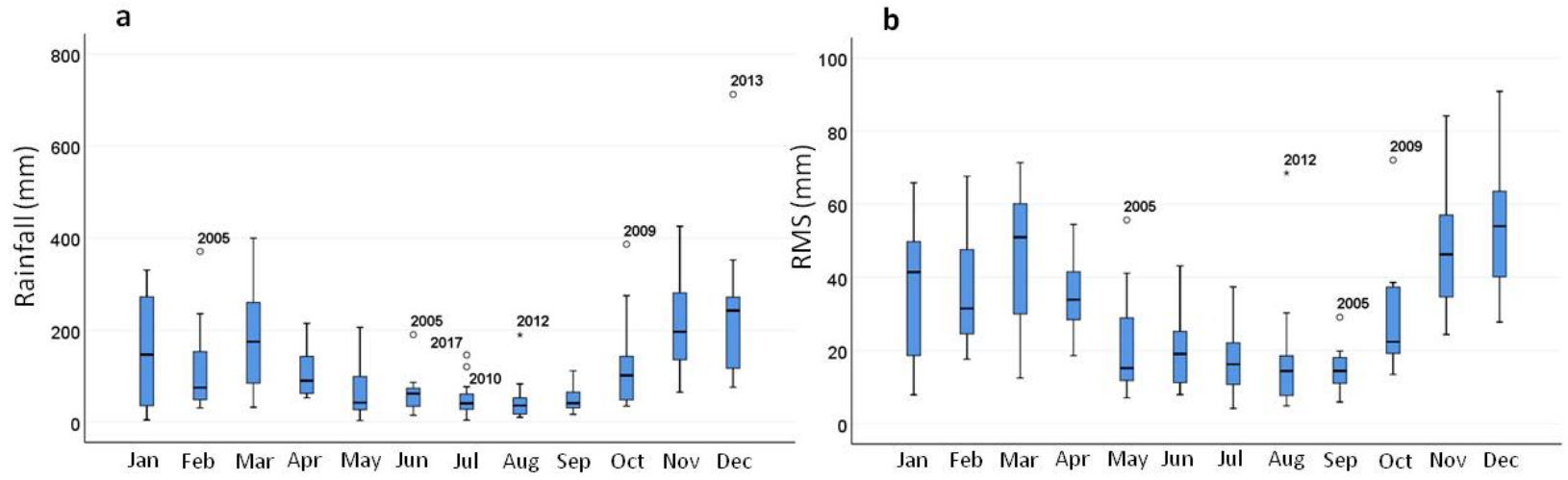
a
Rainfall (mm)
800
600
400
200
0
2005
2005
2017
2010
2012
2009
2013
Jan
Feb
Mar
Apr
May
Jun
Jul
Aug
Sep
Oct
Nov
Dec
b
RMS (mm)
100
80
60
40
20
0
2005
2012
2005
2009
Jan
Feb
Mar
Apr
May
Jun
Jul
Aug
Sep
Oct
Nov
Dec

Figure 3.

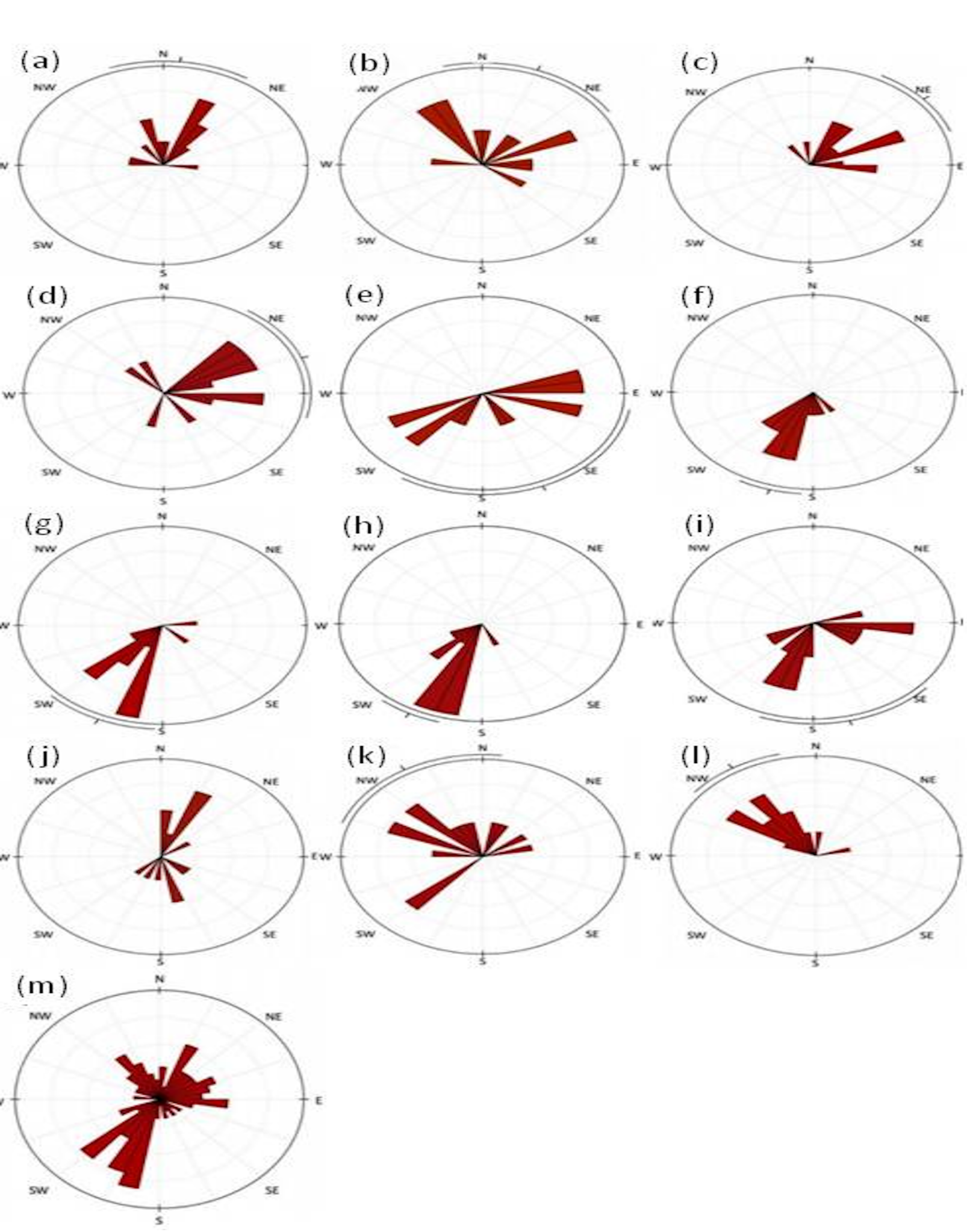
(a)
(b)
(c)
(d)
(e)
(f)
(g)
(h)
(i)
(j)
(k)
(l)
(m)
N
NE
E
SE
S
SW
W
NW

Figure 4.

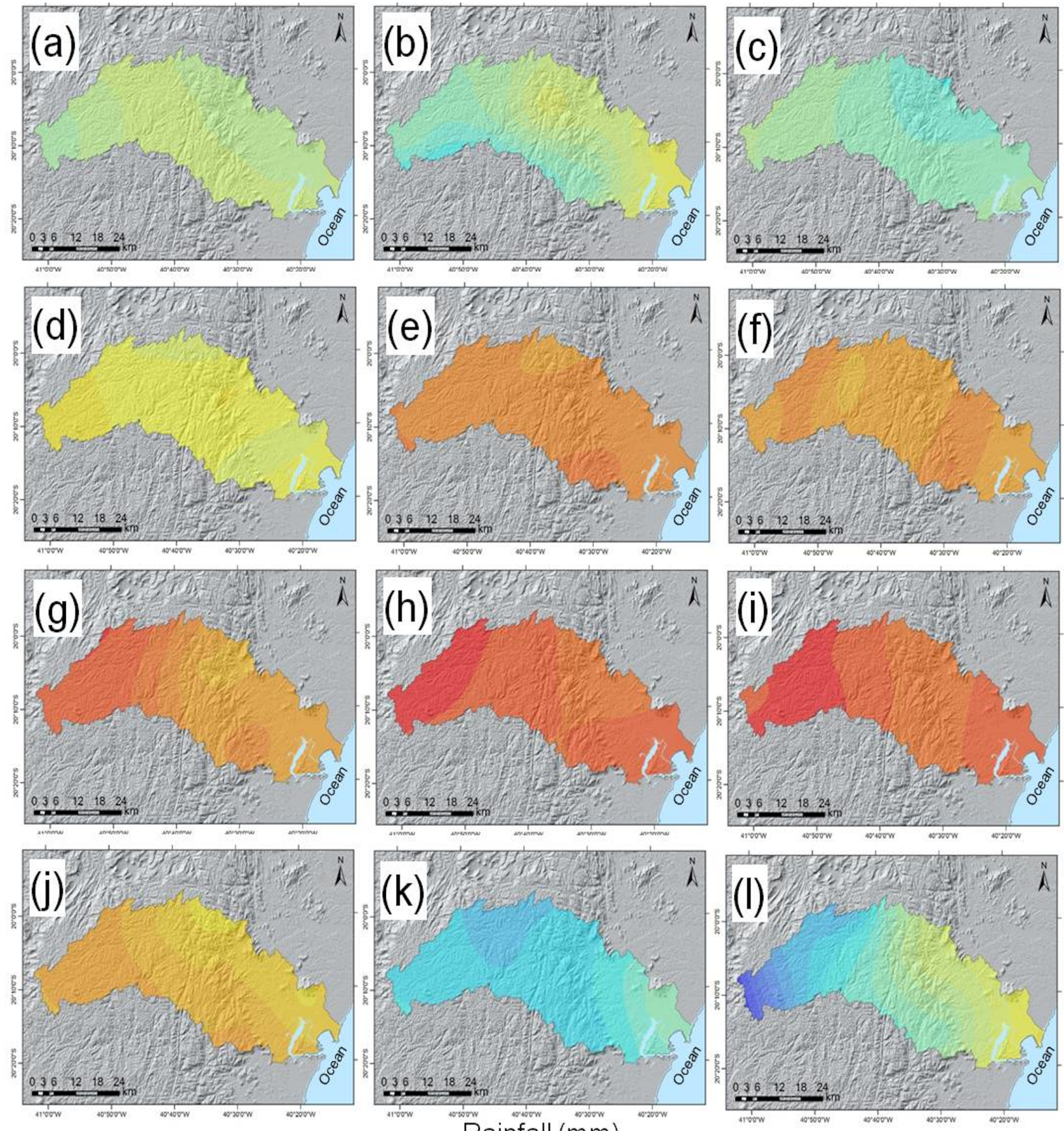
(a)
(b)
(c)
(d)
(e)
(f)
(g)
(h)
(i)
(j)
(k)
(l)
N
0 3 6 12 18 24
km
Ocean
Rainfall (mm)
8
15
30
45
60
75
90
105
120
135
150
165
180
195
210
225
240
255
255
270
285
300
315
330
345

Figure 5.

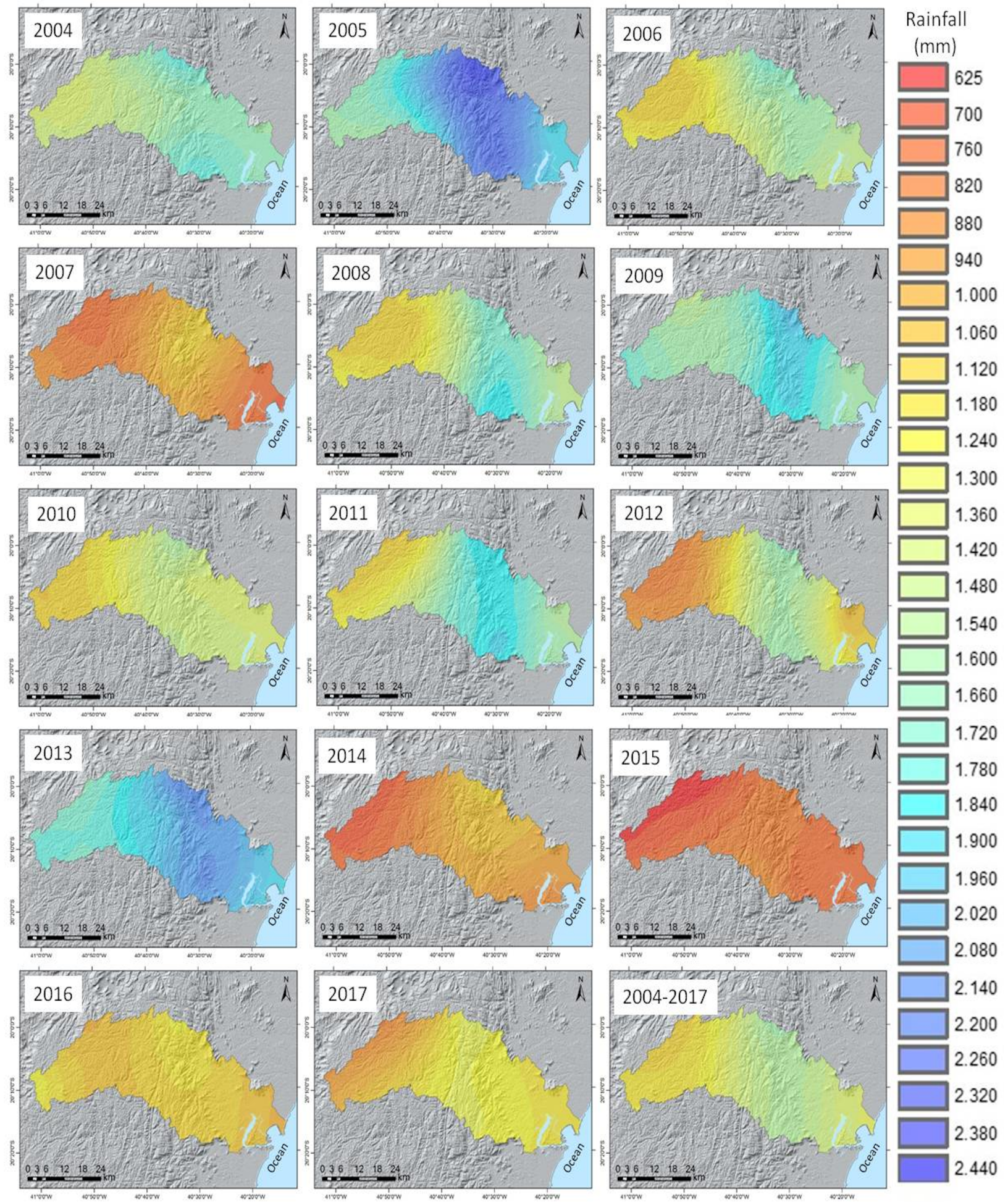
2004
2005
2006
2007
2008
2009
2010
2011
2012
2013
2014
2015
2016
2017
2004-2017
N
0 3 6 12 18 24
km
Ocean
Rainfall (mm)
625
700
760
820
880
940
1.000
1.060
1.120
1.180
1.240
1.300
1.360
1.420
1.480
1.540
1.600
1.660
1.720
1.780
1.840
1.900
1.960
2.020
2.080
2.140
2.200
2.260
2.320
2.380
2.440

Figure 6.

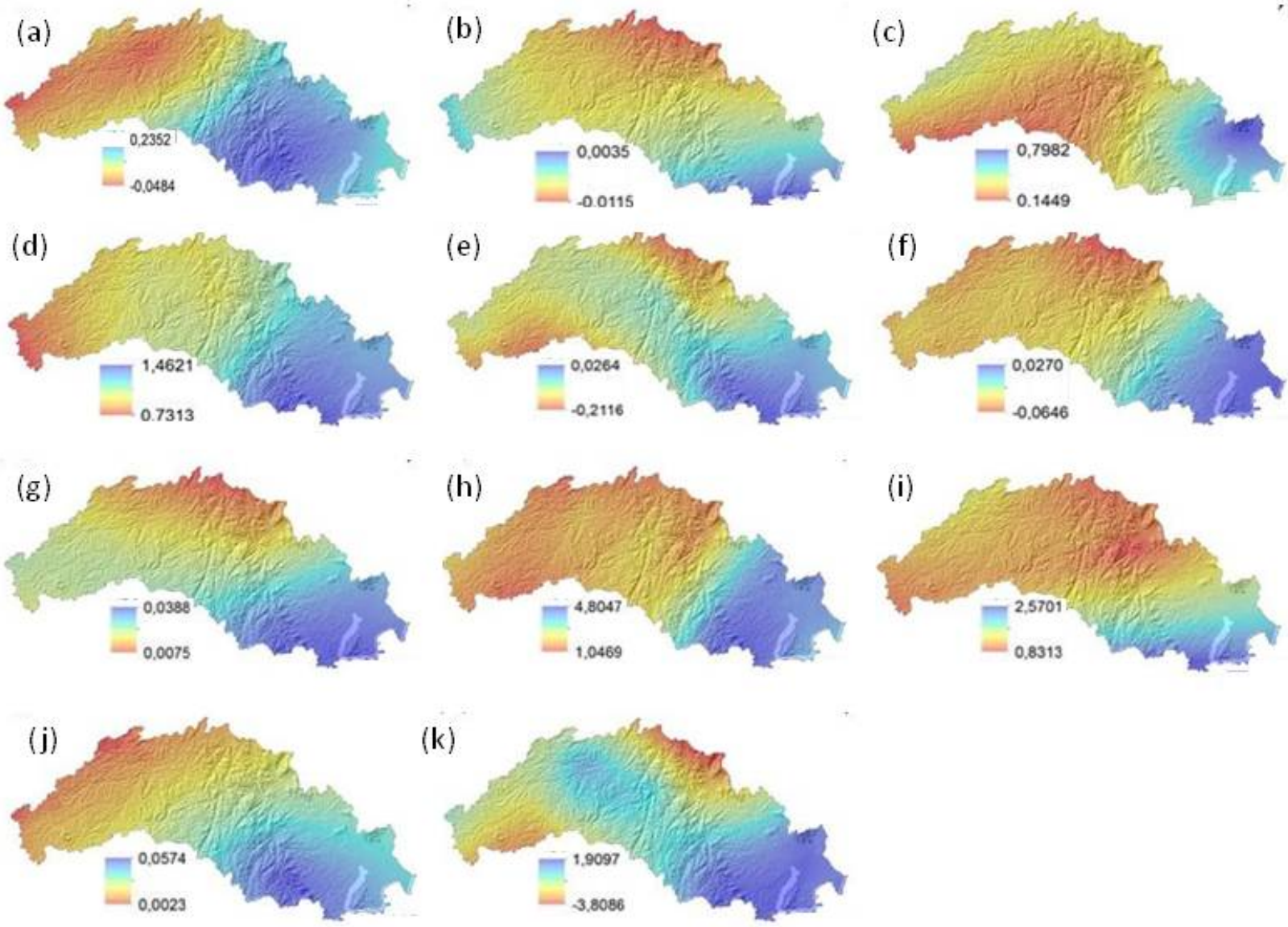
(a)
0,2352
-0,0484
(b)
0,0035
-0.0115
(c)
0,7982
0.1449
(d)
1,4621
0.7313
(e)
0,0264
-0,2116
(f)
0,0270
-0,0646
(g)
0,0388
0,0075
(h)
4,8047
1,0469
(i)
2,5701
0,8313
(j)
0,0574
0,0023
(k)
1,9097
-3,8086

Figure 7.

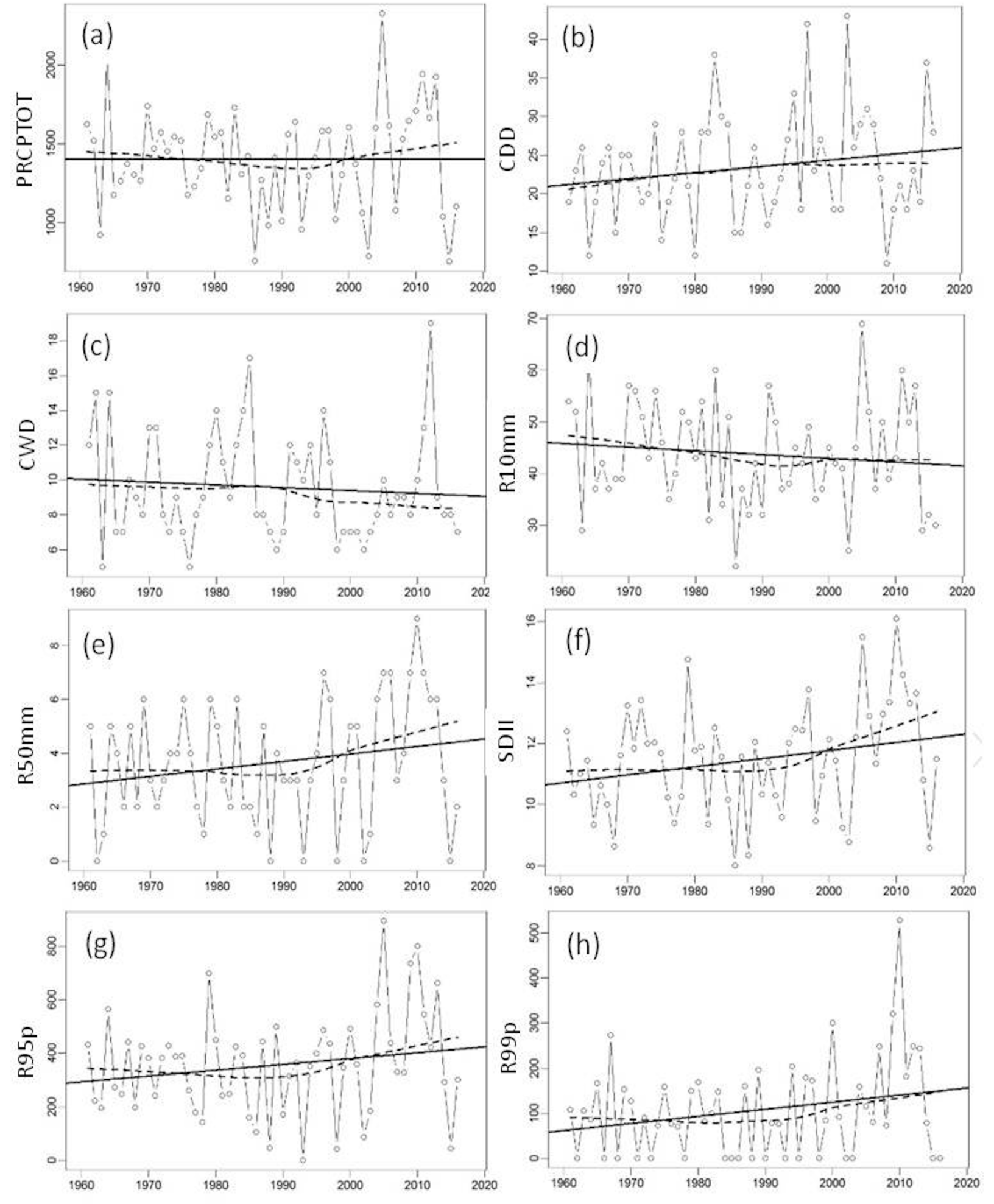
(a)
PRCPTOT
(b)
CDD
(c)
CWD
(d)
R10mm
(e)
R50mm
(f)
SDII
(g)
R95p
(h)
R99p